

Model of Toner Impaction and Developer Failure

Suresh Ahuja, Xerox Corporation Webster NY

Abstract

High definition digital imaging is enabled in printers by using small micron and nano toner particles. Use of small particles in a housing presents challenges in particle flow as small particles tend to aggregate, clog and impact either on the wall of the housing or on other surfaces. Solids are known to undergo brittle- ductile transition depending on the size of a particle, elastic plastic behavior and strain rates under which they are deformed.

In macromolecules, polymer chain flexibility and shear flow of uniformly sized, spherical particles can be analyzed. Inter-particle attractive forces are considered to influence flow of small particles. Simulations performed for different strengths of cohesion, shear rates, particle stiffnesses, particle volume fractions and coefficients of friction show interesting results. From each simulation, the average normal and shear stresses and the average coordination number have been extracted. Generally small particles are externally mixed with nano-sized particles to improve flow. Hard nano-sized particles reduce cohesiveness of toner particles and reduce its aggregation.

Particulate flow can some time result in jamming and has been analyzed using Lattice- Boltzmann (LB) or DEM (Discrete Element Methods) involving deformation from collisions resulting from hydrodynamic forces. Consequence of particle impaction on surfaces is a reduction in particle charge with wider distribution causing shortfalls in electro-photographic development and image quality. A rate equation model is developed for impaction in a cylindrical cavity that depends on the impact parameter, rate of volumetric flow, yield stress (modulus) of the elastic-plastic particle, size of the particle and dynamic coefficient of friction. The model predictions are compared with experimental data on the particle (toner) impaction

Introduction

Powder flow is of industrial importance not only in designing silos and fluidization beds but also in digital imaging using printers and copiers. Toner particles used in digital imaging are 8-10 micron in size with a wide distribution. The flow of polymeric toner particles bound or unbound to carrier beads particles 50-100micron in size takes place through conveyance by augurs in a developer housing to development magnetic rolls. Electric field moves particles from develop roll to photoreceptor. Electric field moves particles from photoreceptor to paper or transparency. Detachment field must overcome toner adhesion to photoreceptor.

The toner particles on paper or transparency as substrate are then fused using contact or non-contact fusing system. The toner particles being micron or sub micron in size can be brittle or ductile during deformation on collisions with carrier beads or surfaces of the cylindrical cavity, developer housing. Particles go through brittle to ductile transition as the particle size is reduced. Additionally, toner particles like other cohesive particles tend to aggregate and invariably clog and jam during transportation [1].

Powders are small granular material in which cohesion is never negligible, and, more particularly in which cohesion forces

are several order of magnitude higher than the weight of the glass beads. The maximum stability angle is found to increase with the powder cohesiveness. There is found a good correlation between bulk stresses and inter-particle contact forces in powders. A common characteristic is that a cohesion force between particles leads to an increase of the avalanche angle of the media. It has been shown that as the cohesion increases, the granular material becomes more heterogeneous, and is made of dense clusters separated by voids. As the cohesion increases, agglomerates of grains increase as transient clusters that leads to a progressive expansion of the material. The analysis of the space and time correlations shows a structural transition above a critical cohesion threshold, associated to a sudden increase of the macroscopic friction. Inter-particle forces (van der Waals, electrostatic, other contact bridging effects from humidity and hydration lead to cohesive forces which can be large compared to gravity acting on the fine particles [2].

Continuum and Discrete Models

Models based on bulk properties including compressibility, cohesion and bulk yield strength are more routinely used as quasi-predictive tools for flow behavior, and are regularly employed in the design and scale-up of industrial unit operations for powder processing as well as overall powder handling systems. Several models have been used to analyze flow of powders.

These include. Lattice - Boltzmann (LB) or DEM (Discrete Element Methods), Particle Dynamics method. In the DEM method, dynamic motion and mechanical interactions between particles arise from collisions, friction, adhesion, and electromagnetic forces [3]. The lattice Boltzmann method LBM, a new method for simulating fluid flow and modeling physics in fluids, has also been successfully applied to flow in porous media. Two approaches have been adopted in simulations of porous flow using LBM.

In the first approach, the fluid in the pores of the medium is directly modeled by the standard LBM. It is well known that unlike the conventional numerical methods based on discretizations of macroscopic continuum equations, LBM is based on microscopic models and mesoscopic kinetic equations for fluids. The kinetic nature of LBM enables it very suitable for fluid systems involving microscopic interactions. Furthermore, the simple bounce-back rule for noslip boundary condition makes it very suitable to simulate the fluid flows in porous media. Gao and Zhao derived LB model by including the porosity into the equilibrium distribution, adding a force term to the evolution equation and solving Navier-Stokes equations for incompressible flow in porous media using Chapman-Enskog procedure. The model was used to give numerical simulations of several 2D generalized Poiseuille flow, Couette flow, and lid-driven cavity flow [4].

The use of the discrete particle model (DPM) enables the simultaneous 'measurement' of several properties, such as the gas and particle velocities. and the porosity, which is difficult if not

impossible to achieve by direct experimentation. The construction of reliable models for large-scale gas–solid contactors is seriously hindered by the lack of understanding of the fundamentals of dense gas–particle flows. In particular, the phenomena which can be related both to the effective gas–particle interaction (drag forces), particle–particle interactions (collision forces), and particle–wall interaction, are not well understood. The prime difficulty here is the large separation of scales: the largest flow structures can be of the order of meters; yet these structures are directly influenced by details of the particle–particle and particle–gas interactions, which take place on the scale of millimeters, or even micrometers[5].

To describe the hydrodynamics of both the gas and particle phase, continuum-(Eulerian) and discrete-(Lagrangian) type of models have been developed. Discrete element models or DPMs have been used for a wide range of applications involving particles. The interaction between the particles and the fluid is done by coupling the DPM with a finite volume description of the gas-phase based on the Navier-Stokes equations for either soft-sphere model or the hard sphere model. These are Euler-Lagrange types of models with discrete description of the particulate phase and a continuous description of gas phase.

Collision Models

In a hard-sphere system the trajectories of the particles are determined by momentum-conserving binary collisions. The interactions between particles are assumed to be pair-wise additive and instantaneous. In the simulation, the collisions are processed one by one according to the order in which the events

occur. For not too dense systems, the hard-sphere models are considerably faster than the soft-sphere models. Note that the possible occurrence of multiple collisions at the same instant cannot be accounted for.

In more complex situations, the particles may interact via short- or long-range forces, and the trajectories are determined by integrating the Newtonian equations of motion. The soft-sphere models use a fixed time step and consequently the particles are allowed to overlap slightly. The contact forces are subsequently calculated from the deformation history of the contact using a contact force scheme.

The soft-sphere models allow for multiple particle overlap although the net contact force is obtained from the addition of all pair-wise interactions. The soft-sphere models are essentially

time driven, where the time step should be carefully chosen in the calculation of the contact forces. The soft-sphere models that can be found in literature mainly differ from each other with respect to the contact force scheme that is used.

The motion of every individual element is calculated using Newton's second law of motion. The forces considered are from pressure gradient, drag, gravity, contact forces arising from collisions and (long-range) particle–particle interaction Van der Waals forces).

Using a governing equation for discrete particles, drag force was derived by Beestra [6].

$$F = \frac{\beta d_p^2}{\mu} = A \frac{\varepsilon_s^2}{\varepsilon_g} + B \varepsilon_s Re \quad (1)$$

$$A = 180 + \frac{18 \varepsilon_g^4}{\varepsilon_s} (1 + 1.5 \sqrt{\varepsilon_s}) \quad (2)$$

$$B = \frac{0.31(\varepsilon_g^{-1} + 3\varepsilon_g \varepsilon_s + 8.4 Re^{-0.343})}{1 + 10^{3\varepsilon_s} Re^{2\varepsilon_g - 2.5}} \quad (3)$$

In the above equations, the terms d is the particle diameter, μ is dynamic coefficient of friction, ε is the dimensionless volume fraction and Re is the Reynold's number. The gas-phase hydrodynamics are calculated from the volume-averaged Navier–Stokes equations.

The equations for the gas-phase are coupled with those of the particle phase through the porosity and the inter-phase momentum exchange. All relevant quantities should be averaged over a volume, which is large compared to the size of the particles, and in such a way that they are independent of the Eulerian grid size.

Porosity and the force exerted by the gas-phase on the particles may be calculated in a grid-independent manner where particles are represented as porous cubes, where this geometry was selected because of its computational advantages. The diameter of the cube depends on the particle diameter and a constant scaling factor a , which defines the ratio between the cube and particle diameter and consequently the volume where interaction between the fluid and the particle is considered.

Iordanoff et al.[7] described recent approaches for modeling the behavior of third bodies in dry contact. His analysis of existing models showed that mathematical modeling of powders falls into two general classes, discrete models and continuum models. According to Iordanoff, discrete models suffer from inadequate understanding of interaction laws, questionable definition of particle scale, and huge computational times. On the other hand, while continuum models are computationally much simpler, they usually are limited to two-dimensional kinetics. In the flow factor model of Jeng and Tsai [8], grain-grain collisions and roughness are considered deriving flow rate volumes for elastic and inelastic grain collisions. The normal stress for top smooth and rough surfaces was expressed as a function of the nominal shear rate and normal stress increases with increasing nominal shear rate and inclination of the upper surface for the smooth surface. The model showed that larger particle size and smaller collision energy loss contribute to significant roughness effects in grain flow lubrication.

In a sheared granular flow of rough inelastic granular particles in a cylindrical cavity, collision between particle and wall can be inelastic if contact stress exceeds yield stress of the particle. If the coefficient of restitution, $\varepsilon = 0$, the particle will stick to the wall, where as, for $\varepsilon = 1$, the collision is elastic and particle has no loss in energy on impact.

Consider a collision between two particles with precollisional linear velocities \mathbf{u} and \mathbf{u}^* and angular velocities $\boldsymbol{\omega}$ and $\boldsymbol{\omega}^*$,

such that the unit vector along the line joining the centers of the particles is \mathbf{k} . The precollisional relative velocity at the point of contact is

$$\mathbf{g} = [\mathbf{u} + (\sigma \mathbf{k} / 2) \times \boldsymbol{\omega}] - [\mathbf{u}^* - (\sigma \mathbf{k} / 2) \times \boldsymbol{\omega}^*] \quad (4)$$

The collision rules stipulate that the post-collisional relative velocity at the point of contact \mathbf{g}' is related to the pre-collisional relative velocity \mathbf{g} by

$$\mathbf{g}'_n = -e_n \mathbf{g}_n \quad \mathbf{g}'_t = -e_t \mathbf{g}_t \quad (5)$$

where \mathbf{g}_n and \mathbf{g}'_n are the components of \mathbf{g} in the direction of \mathbf{k} , \mathbf{g}'_t and \mathbf{g}_t are the components of \mathbf{g} perpendicular to the direction of \mathbf{k} and e_n and e_t are the normal and tangential coefficient of restitution [9]. Analytical results were obtained for the velocity distribution function for collisions of smooth particles by Kumaran [10] using an asymptotic analysis in the small parameter $\varepsilon = n \sigma L$, which is proportional to the inverse of the Knudsen number, where n is the number density, σ is the diameter of the particle, and L is the channel width. For sheared granular flows in the high Knudsen number limit, the frequency of wall-particle collisions per unit area [11] is proportional to $n u_y / L$, whereas the number of interparticle collisions is proportional to $n^2 \sigma (u_x^2 + u_y^2)^{1/2}$ subscripts x and y stand for flow and gradient directions.

The flow of a collection of polymer-coated metal sphere in a tubular flow was analyzed analytically by considering a single inelastic collision as an elastic-plastic collision with plastic deformation resulting in adhesion to an impacting surface [12,13]. The amount impacted in a single collision was combined with collision frequency to obtain a rate equation. The results showed that the amount impacted on a surface depends directly on fluid flow velocity, density of the particle and radius of the particle.

In a discrete numerical model for granular assemblies that can be applied to flow of toner particle, collisions between toner particles can be normal or tangential. A normal collision between two objects is characterized by the normal coefficient of restitution and the contact time. The normal coefficient of restitution is determined experimentally. The collision time is estimated from the collision theory of Hertz. In tangential collisions, shear contact force component F_s , being the component in s -direction of the contact force on particle was modeled with a Coulomb friction mode. The friction model for tangential collision is characterized by three parameters: the static and dynamic friction coefficient and the tangential spring constant. Adhesion force, Magnetic force, Electric force were included in the simulation [14,15].

It is known that particles made from a polymer undergo brittle to ductile transition. Below a certain molecular weight, a polymer is brittle and deforms in ductile fashion. Additionally, a polystyrene polymer is brittle while a polycarbonate polymer is ductile. A particle below a certain size generally below a micron is ductile while it is brittle above that size. In Chang et. al. model [16] the sphere remains in elastic Hertzian contact until a critical interference is reached, above which volume conservation of the sphere tip is imposed. The contact pressure distribution for the plastically deformed sphere was assumed to be rectangular and equal to the maximum Hertzian pressure at the critical interference. The CEB model suffers from a discontinuity in the contact load as well as in the first derivatives of both the contact

load and the contact area at the transition from the elastic to the elastic-plastic regime.

Works of Nesterenko et al. [17] and Zhodi [18] showed that particles as spheres may adhere to one another, forming branched aggregates with a transition from size-unstable agglomeration to size-stable agglomeration, which is controlled by the velocity field and the material properties. Toner particles may also form aggregates through collisions in a cavity with a criterion that adhesion of two surfaces occurs when $p > 2H$, where H is the hardness of the material. Contact pressure relates to the coefficient of restitution by a linear interpolation model between elastic ($e = 1$) and adhesive ($e = 0$) conditions.

Contact area A can be taken to be a decreasing function of e . A linear relation for A in terms of e can be used.

$$e = \max \left\{ 1 - \frac{p}{2H}, 0 \right\} = \max \left\{ 1 - \frac{|P_{nor}|}{HA \delta t}, 0 \right\} \quad (6)$$

$$A = (A_0 + (A_f - A_0)(1 - e)) \rho \quad (7)$$

Dependence of impaction of toner aggregates to the housing cavity was verified experimentally to depend on hardness. As the toner particles from resin were melt mixed with ferrite, iron oxide hard particles, aggregate sticking decreased. On the contrary as the flow rate of toner aggregates was increased, sticking of aggregates to the cavity increased.

Toner particles 10 micron in size were mixed with carrier beads 250 micron in size and sheared in a cylindrical cavity with the help of augurs. Toner impaction was obtained by removing the loose particles from carrier beads and then transferring stuck toner.

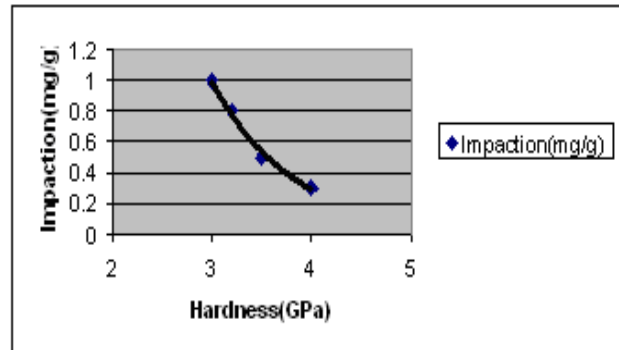


Figure 1 - shows toner impaction as function of toner (particle) hardness.

Toner particles may form aggregates and collide with other aggregates or with surfaces of other materials. Using elastic-plastic analysis of Jackson and Green [19] for a deformable toner particle sphere pressed by a rigid flat surface of a cylindrical cavity, critical interference ω_c , critical contact force P_c and critical contact A_c area can be calculated.

$$\omega_c = \left(\frac{\pi C S_y}{2 E'} \right)^2 R \quad (8)$$

$$P_c = \frac{4}{3} \left(\frac{R}{E'} \right)^2 \left(\frac{C}{2} \pi S_y \right) \quad (9)$$

$$A_c = \pi^3 \left(\frac{C S_y R}{2 E'} \right)^2 \quad (10)$$

where C is a critical yield stress coefficient dependent on the Poisson's ratio, of the toner material in the neighborhood of 0.33 and S_y is the yield strength 40MPa. Experiments on toner impactation by mixing toner particles with carrier beads in a cylindrical cavity showed that impactation, impactation is quadratically dependent on radius of toner particle.(Figure 2)

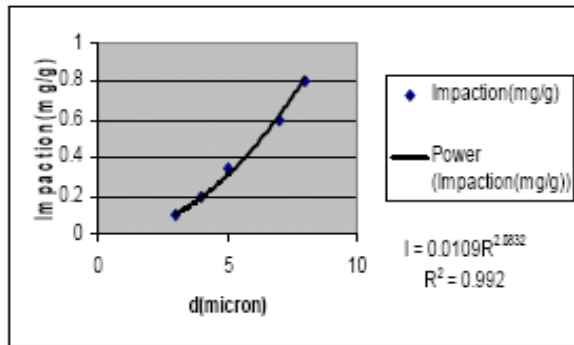


Figure 2 shows the dependence of impactation on toner radius

The impactation rate is proportional to the energy exchange between the erodent and the impacted material surface. Different particles transfer the energy to the target over a different volume, thereby causing different energy densities in the target material and different mechanisms and rates of damage. The solution lies in calculation of the energy, absorbed by the plain material surface during the impact of a spherical particle. Energy loss strongly depends on dynamic coefficients, on the coefficient of velocity restitution after impact, and coefficient of dynamic friction. For particle wall collisions, kinetic energy loss can be given by [20],

$$K = \frac{1}{2} m v_{n_1}^2 (1 + k) \left[1 - k + 2fb - f^2(1 + k)(1 + \lambda) \right] \quad (11)$$

Where K is kinetic energy loss. v_{n_1} is the normal component of particle velocity, k is the coefficient of restitution of the normal component of velocity, f is the tangential velocity restitution or coefficient of dynamic friction, for a solid sphere $\lambda = 5/2$ and b is

$$b = \frac{(v_{n_1} - R\omega)}{v_{n_1}}$$

Experiments on toner particles mixed with carrier beads showed that impactation was dependent on square of the flow velocity

In a recent patented work by Hamby et al., a method for sensing toner concentration in a developer housing was found for

compensating optical measurements of toner concentration for toner impactation. The method involved sensing the light reflected of the developer material with optical system and getting toner concentration from the reflected light off the developer material [21]. Experimental results showed that toner impactation (mg/g) is

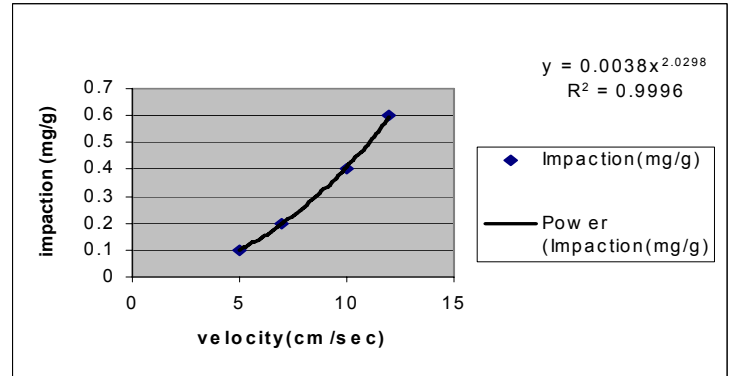


Figure 3 – shows toner impactation is dependent on the square of flow velocity

correlated to carrier age in thousands of prints. Increasing toner hardness, decreasing toner size and lowering of flow velocity would result in reduction of toner impactation and increase in carrier age.

CONCLUSION

Analytical and numerical models for toner (particle) impactation are considered. The models predict dependence on coefficient of restitution, hardness and pressure. Impactation of toner (particle) aggregates is consistent with experimental data on particle radius.

Acknowledgment

Support from Xerox over many years was critical for this work

References

- [1] Valverde, J.M. Castellanos, A., Ramos, A., Physical Review **E62**-5 6851-68 (2000)
- [2] Castellanos, A., Valverde, J., Perez, A., Ramos, A. and Watson, P., Phys. Rev. Lett. **82**, 1156–1159(1999).
- [3] Wolf, D.E., Computational Physics, 64-94(1996)
- [4] Guo, Z., Zhao, T. S., Physical Review **E 66**, 036304 1 -9(2002)
- [5] Deen N.G., Sint Annaland, M., Van der Hoef M.A., Kuipers J.A.M., Chemical Engineering Science 62, 28 – 44(2007)
- [6] Beetstra, R., Van der Hoef, M.A., Kuipers, J.A.M, Chemical Engineering Science, the special issue on Fluidized bed applications (2006)
- [7] Iordanoff, I., Berthier, Y., Descartes, S., and Heshmat, H., 2002, ASME J. Tribol., **124**, pp. 725–735. (2002)
- [8] Jeng, Y.-R., Tsai H., ASME J. Tribol., **127**, 837-844(2005)
- [9] Lun, C. K. K, J. Fluid Mech. 233, 539 (1991)
- [10] Kumaran, V. J. Fluid Mech. 340, 319 (1997).
- [11] Kumaran, V., PRL 95, 108001 (2005)
- [12] Levich, V. G., "Hydrodynamics," Prentice Hall, Englewood Cliffs, N.J., 1962
- [13] Ahuja, S.K., J. Coll. Interface Sc., 57, 438-445(1976)
- [14] Cundall, P.A. and Strack, O.D.L, Geotechnique **29**, 47 (1979)

- [15] Severens, I. E.M, van de ven A. A. F, Wolf, DE, Mattheij, R.M.M, *Granular Matter*,8,3(4)137-150(2006)
- [16] Chang, W. R., Etsion, I., and Bogy, D. B., *ASME J. Tribol.*, **109**, 257–263 (1987)
- [17] Nesterenko, V. F., Meyers, H. C. Chen, M. A. and LaSalvia. J. C., *Applied Physics Letters*, 65 (24), 3069-3071(1994).
- [18] Zohdi. T. I., *International Journal of Nonlinear Mechanics*, 38 (8), 1205-1219, 2003.
- [19] Jackson R L. and Green, I., *ASME J.Tribol.*,**127**,343-354(2005)
- [20] Hussainovaa, I., Schade K and Tisler S., *Proc. Estonian Acad. Sci. Eng.*, **12**, 1, 26–3992006).
- [21] Hamby et al., *US Patent Application Publication US* 2004/02649859(2004)

Author Biography

Suresh Ahuja received his BS in physics and chemistry from the Punjab University (1959), his MS in Soil Physics from Indian Research Institute (1961) and his PhD in Polymer Physics from Polytechnic Institute of Brooklyn (1967). After working over 37 years at Xerox with several years as Principal Scientist he retired. He has several patents including three this year. He has published over 70 publications and presentations at international conferences. He is a member of APS, ASME, SOR and IST.